JOURNAL OF ENVIRONMENTAL SCIENCES 117 (2022) 151–160

Available online at www.sciencedirect.com

ScienceDirect

www.elsevier.com/locate/jes

JES JOURNAL OF ENVIRONMENTAL SCIENCES

www.jesc.ac.cn

Formation of regulated and unregulated disinfection byproducts during chlorination and chloramination: Roles of dissolved organic matter type, bromide, and iodide

Yunsi Liu [1,2], *Keqiang Liu* [3], *Michael J. Plewa* [4], *Tanju Karanfil* [5], *Chao Liu* [1,2,*]

[1] *Key Laboratory of Drinking Water Science and Technology, Research Center for Eco-Environmental Sciences, Chinese Academy of Sciences, Beijing 100085, China*

[2] *University of Chinese Academy of Sciences, Beijing 100049, China*

[3] *Water Conservancy Development Research Center, Taihu Basin Authority, Ministry of Water Resources, Shanghai 200433, China*

[4] *Department of Crop Sciences, and the Safe Global Water Institute, University of Illinois at Urbana-Champaign, Urbana, IL 61801, USA*

[5] *Department of Environmental Engineering and Earth Sciences, Clemson University, Anderson, SC 29625, USA*

ARTICLE INFO

Article history:
Received 28 February 2022
Revised 8 April 2022
Accepted 9 April 2022
Available online 19 April 2022

Keywords:
Disinfection byproducts
Natural organic matter
Algal organic matter
Effluent organic matter
Bromide
Iodide
Chlorination
Chloramination

ABSTRACT

Algal blooms and wastewater effluents can introduce algal organic matter (AOM) and effluent organic matter (EfOM) into surface waters, respectively. In this study, the impact of bromide and iodide on the formation of halogenated disinfection byproducts (DBPs) during chlorination and chloramination from various types of dissolved organic matter (DOM, e.g., natural organic matter (NOM), AOM, and EfOM) were investigated based on the data collected from literature. In general, higher formation of trihalomethanes (THMs) and haloacetic acids (HAAs) was observed in NOM than AOM and EfOM, indicating high reactivities of phenolic moieties with both chlorine and monochloramine. The formation of haloacetaldehydes (HALs), haloacetonitriles (HANs) and haloacetamides (HAMs) was much lower than THMs and HAAs. Increasing initial bromide concentrations increased the formation of THMs, HAAs, HANs, and HAMs, but not HALs. Bromine substitution factor (BSF) values of DBPs formed in chlorination decreased as specific ultraviolet absorbance (SUVA) increased. AOM favored the formation of iodinated THMs (I-THMs) during chloramination using preformed chloramines and chlorination-chloramination processes. Increasing prechlorination time can reduce the I-THM concentrations because of the conversion of iodide to iodate, but this increased the formation of chlorinated and brominated DBPs. In an analogous way, iodine substitution factor (ISF) values of I-THMs formed in chloramination decreased as

* Corresponding author.
E-mail: chaoliu@rcees.ac.cn (C. Liu).

https://doi.org/10.1016/j.jes.2022.04.014

SUVA values of DOM increased. Compared to chlorination, the formation of noniodinated DBPs is low in chloramination.

Introduction

Due to population growth and frequent anthropogenic activities, natural waters have been influenced by harmful algal blooms (HABs) (Chapra et al., 2017) and the discharge of municipal wastewater effluents (Chuang and Mitch, 2017), resulting in variable dissolved organic matter (DOM) constituent in water and posing challenges to potable water supply. Natural organic matter (NOM) mostly derived from lignin is enriched in aromatic phenolic structures (Leenheer and Croué, 2003). However, in HAB events, algal organic matter (AOM), comprising proteins, carbohydrates, lipids, nucleic acids, and biopolymers, can be released into drinking water during algal cells growth and lysis naturally or chemically (Henderson et al., 2008; Lee and Westerhoff, 2006). In addition, wastewater treatment plants (WWTPs) can introduce effluent organic matter (EfOM) consisting of variable compounds into the downstream surface waters, which includes NOM from drinking water, synthetic organic chemicals from anthropogenic use and soluble microbial products (SMPs) and extracellular polymeric substances (EPS) from biological treatment processes (Shon et al., 2006; Sirivedhin and Gray, 2005). AOM and EfOM exhibit more hydrophilic characters and a higher ratio of dissolved organic nitrogen (DON) to dissolved organic carbon (DOC) and less aromatic carbon content (Henderson et al., 2008; Her et al., 2004; Westerhoff and Mash, 2002). As a result, this hydrophilic organic carbon fraction is less prone to coagulation, sedimentation and sand filtration processes (Lee and Westerhoff, 2006; Widrig et al., 1996). The fraction of AOM and EfOM over the bulk DOM may increase before disinfection process (Aziz et al., 2022; Eom et al., 2017).

Disinfection is an efficacious safeguard of drinking water quality. Chlorine is the most used disinfectant globally for its low-cost and ability to maintain residual disinfectant in distribution systems (Liu, 2021). Toxic disinfection by-products (DBPs) can be however produced unintendedly from the reaction of chlorine and DOM in water (Bellar et al., 1974; Rook, 1974). Regulated DBPs, e.g., trihalomethanes (THMs) and haloacetic acids (HAAs), are the most prevalent species in disinfected waters (USEPA, 2006; WHO, 2006). In recent years, haloacetaldehydes (HALs), as the third most abundant DBPs (Krasner et al., 2006; Richardson et al., 2007), have also been included in drinking water standards in some countries such as China, Japan and Korea (Ministry of Health of the PR China, 2022; Ministry of Health of Japan, 2015; Ministry of Environment of Korea, 2020). They exhibited higher cytotoxicity index values (CTI) compared with THMs and HAAs (Jeong et al., 2015). In addition, though nitrogenous DBPs (N-DBPs), e.g., haloacetonitriles (HANs) and haloacetamides (HAMs), typically occur at lower concentrations in drinking water than regulated THMs and HAAs, their formation is of concern since their high cytotoxicity and genotoxicity may offset these concentrations (Muellner et al., 2007; Plewa et al., 2010; Wei et al., 2020). Furthermore, drinking water providers are increasingly relying on algal- and wastewater-impacted sources, which are characterized by a higher organic nitrogen content that is a known precursor for these N-DBPs (Mitch et al., 2009).

In the presence of bromide (Br^-) and iodide (I^-), chlorine (in the form of hypochlorous acid, HOCl) can oxidize Br^- and I^- to hypobromous and hypoiodous acids (i.e., HOBr and HOI, respectively) (Kumar and Margerum, 1987), which can further react with DOM to form brominated and iodinated DBPs (Br-DBPs and I-DBPs, respectively). As elevated halide levels are being reported in surface waters due to industrial wastewater discharge, hydraulic fracturing and saltwater intrusion (Elimelech and Phillip, 2011; Good and VanBriesen, 2016; Watson et al., 2012), increasing bromine incorporation into formed DBPs during chlorination process has been observed in recent years. Since chlorine can further oxidize HOI to nontoxic iodate (IO_3^-), IO_3^- is the main sink in chlorination process (Liu et al., 2014). On the contrary, chloramines can rapidly oxidize I^- to hypoiodous acid (HOI) but do not further oxidize HOI to the nontoxic iodate, leading to the formation of I-DBPs. The formation of Br-DBPs and I-DBPs is of particular concern because they exhibit higher cytotoxicity and genotoxicity than their corresponding chlorinated analogues (Plewa et al., 2010; Richardson and Plewa, 2020; Richardson et al., 2007).

The effects of bromide and iodide ions on the formation of various DBPs during chlorination and chloramination have been extensively studied (Allard et al., 2015; Ersan et al., 2019a; Ersan et al., 2019b; Hua et al., 2006; Jones et al., 2012; Liu et al., 2018, 2019). Our previous study indicated that increasing initial Br^- concentrations increased the formation of THMs and HANs, while concentrations of HAAs remained stable during chlorination of algal-impacted waters (Liu et al., 2018). Of note, previous studies from various publications were conducted at distinct experimental conditions, rendering it difficult to compare the DBP formation from different origins side by side. In addition, the understanding of how does bromine and iodine incorporation to DOM from various origins differ in terms of DBP formation and speciation remains unknown.

The objectives of this study are to compare the formation and speciation of various DBPs (i.e., THMs, HAAs, HANs, HALs and HAMs) from different DOM origins with varying bromide/iodide levels from literature under simulated distribution system conditions when data are available. Three disinfection processes include chlorination, chloramination with preformed chloramine and prechlorination followed by ammonia addition. Based on the information of DBPs collected from literature, bromine/iodine substitution factors were calculated and linear regression analy-

ses between DBP formation and water characteristics were performed.

1. Materials and methods

1.1. Data compilation

1.1.1. THMs, HAAs and HANs

A comprehensive DBP database for THMs, HAAs and HANs was collected from the literature (Appendix A Tables S1-S3). For the selected database, water samples were treated in similar disinfection conditions, i.e., HOCl dose/DOC ratio at 1.4–3.3 mg Cl_2/ mg C of pH 7–8, contact time = 24 hr, and temperature = 20–25 °C. Of note, samples in the dataset covered a wide range of $SUVA_{254}$ (0.5–5.4 L/(mg•m)) and DOC (0.9–10.5 mg/L). The chosen ratio of chlorine/chloramine dose and DOC ensured the presence of a measurable residual in samples after 24 hr (Cowman and Singer, 1996). Elevated free chlorine levels can result in decomposition of some DBPs (Kanan and Karanfil, 2020). To investigate the effect of initial Br^- concentration on the DBP formation during chlorination, various Br^- concentrations were normalized with the DOC concentration. The $[Br^-]$/DOC mass ratios were divided into five groups: Ambient (0–0.01), 0.03 (0.02–0.04), 0.1 (0.06–0.14), 0.2 (0.16–0.31) and 0.4 (0.36–0.44). For each group, the value represents the mean.

Since I-DBPs can be formed during chloramination, the effect of initial I^- concentration on DBP formation was investigated in chloramination with preformed chloramine and prechlorination followed by ammonia addition processes. The $[I^-]$/DOC mass ratios were divided into five groups as well: Ambient (0–0.006), 0.014 (0.010–0.017), 0.035 (0.030–0.040), 0.055 (0.047–0.063) and 0.400. For each group, the value represents the mean. The dataset included the results for samples from laboratory-cultured AOM samples ($n = 16$, chlorination; $n = 10$, chloramination), NOM samples ($n = 89$, chlorination; $n = 45$, chloramination) and EfOM samples from secondary effluents of different WWTPs ($n = 23$, chlorination; $n = 2$, chloramination). For prechlorination conditions, 36 AOM samples and 31 NOM samples were collected owing to the limited data available.

The water quality parameters of samples containing different types of DOM sources are shown in Appendix A Tables S1–S3, supplementary information. Four THMs (chloroform (TCM), bromodichloromethane (BDCM), dibromochloromethane (DBCM), and bromoform (TBM)), nine HAAs (monochloro-, dichloro-, trichloro-, monobromo-, dibromo-, bromochloro-, bromodichloro-, dibromochloro-, and tribromo-acetic acids (MCAA, DCAA, TCAA, MBAA, DBAA, BCAA, BDCAA, DBCAA, and TBAA, respectively)), six I-THMs (dichloroiodomethane (DCIM), bromochloroiodomethane (BCIM), dibromoiodomethane (DBIM), chlorodiiodomethane (CDIM), bromodiiodomethane (BDIM), and iodoform (TIM)), six HANs (monochloro-, dichloro-, trichloro-, monobromo-, dibromo-, and bromochloro-acetonitrile (CAN, DCAN, TCAN, BAN, DBAN, and BCAN, respectively) were investigated.

1.1.2. HALs and HAMs

Separate databases for HAL and HAM formation were collected from the literature (Appendix A Tables S4–S6) due to the difficulties to keep identical experimental conditions with THMs, HAAs and HANs. Formation of HALs were collected from water samples (26 AOM, 9 NOM and 2 EfOM samples) with ranges of $SUVA_{254}$ (0.4–4.3 L/(mg•m)) and DOC (2.0–6.8 mg/L). Samples covered a range of pH (7.0–7.7), HOCl dose/DOC ratio (0.7–3.2 mg Cl_2/ mg C), contact time (24–168 h), and temperature (20–25 °C).

For HAMs, the dataset for chlorination covered a range of $SUVA_{254}$ (0.4–8.8 L/(mg•m)), DOC (1.5–13.4 mg/L), DON (0.02–4.30 mg/L), pH (6.9–8.0), HOCl dose/DOC ratio (1.1–9.8 mg Cl_2/mg C), contact time (2–72 hr), and temperature (20–25 °C). The dataset included 2 AOM, 24 NOM and 13 EfOM samples. The dataset for chloramination covered a range of $SUVA_{254}$ (0.4–8.8 L/(mg•m)), DOC (1.5–13.4 mg/L), DON (0.02–1.51 mg/L), pH (6.9–8.0), NH_2Cl dose/DOC ratio (1.0–5.0 mg Cl_2/ mg C), contact time (0.5–72 hr), and temperature (20–25 °C). The dataset included 2 AOM, 25 NOM and 8 EfOM samples.

The water quality parameters of samples containing different types of DOM sources are shown in Tables S4–S6, supplementary information. Four HALs (trichloro-, bromodichloro-, dibromochloro-, and tribromoacetaldehyde (TCAL, BDCAL, DBCAL, and TBAL, respectively)) and four HAMs (dichloro-, trichloro-, dibromo-, and bromochloroacetamide (DCAM, TCAM, DBAM, and BCAM, respectively)) were investigated.

1.2. Calculation of bromine/iodine substitution factors

Bromine substitution factor (BSF) was calculated as Eq. (1) and defined as the ratio of the molar concentration of bromine incorporated into a given class of DBP to the total molar concentrations of chlorine and bromine in that class (Hua et al., 2006).

$$BSF = \frac{\sum Br_{DBP}}{\sum Br_{DBP} + \sum Cl_{DBP}} \quad (1)$$

Taking THM as an example, BSF_{THM} was calculated as Eq. (2).

$$BSF_{THM} = \frac{BDCM + 2DBCM + 3TBM}{3(TCM + BDCM + DBCM + TBM)} \quad (2)$$

Iodine substitution factor (ISF) is defined as the ratio of the molar concentration of iodine incorporated into a given class of DBPs to the total molar concentrations of chlorine, bromine and iodine in that class (Liu et al., 2019). When THM (10 species, including six I-THMs and THM4) was used as an example, molar concentrations of iodine and sum of chlorine, bromine and iodine could be calculated by Eqs. (3) and (4), respectively, where THM10 is sum of 10 species of THMs. ISF of THM can be calculated by Eq. (5).

$$\sum I_{THM} = [DCIM] + [BCIM] + [DBIM] + 2[CDIM] + 2[BDIM] + 3[TIM] \quad (3)$$

$$\sum Cl_{THM} + Br_{THM} + I_{THM} = 3[THM10] \quad (4)$$

$$ISF_{THM} = \frac{\sum I_{THM}}{3[THM10]} \quad (5)$$

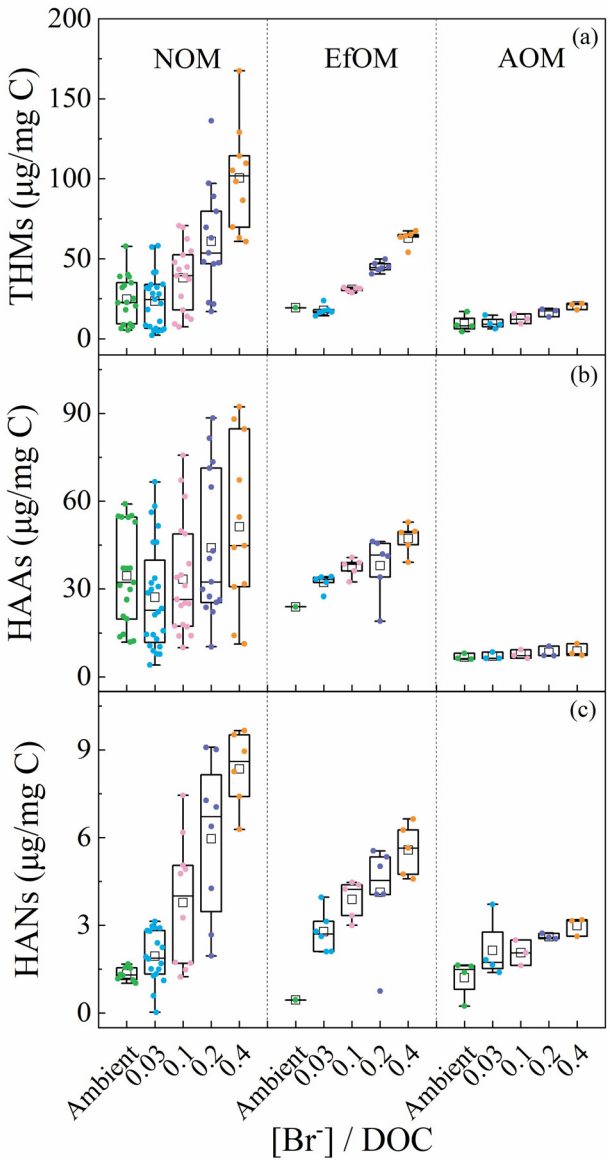

Fig. 1 – Statistical analyses for the yields of total (a) THMs, (b) HAAs and (c) HANs during chlorination of NOM, EfOM, and AOM samples under various initial Br^- concentrations from literature. Conditions: [HOCl]/DOC = 1.4–3.3 mg Cl_2/mg C, pH = 7–8, T = 20–25 °C, reaction time = 24 hr.

2. Results and discussion

2.1. *DBP formation during chlorination*

2.1.1. *THMs*

As shown in Fig. 1a, total THM yields of NOM samples were significantly higher than EfOM and AOM in most cases. For example, when the initial Br^- concentrations in various types of water were in a low range (ambient level to [Br^-]/DOC of 0.03), THM yields were 4.6–58.1, 14.3–23.8, 6.2–17.0 μg/mg C for NOM, EfOM, and AOM, respectively. The median level of THM yields at [Br^-]/DOC of 0.03 were 24.6, 17.0 and 8.90 μg/mg C for NOM, EfOM, and AOM, respectively, which was associated with their SUVA values . It has been reported that increasing the aromaticity of DOM (i.e., SUVA) enhanced the formation of THMs (Liu and Croué, 2016).

Increasing the initial Br^- concentration increased the formation of total THMs (Fig. 1a), in line with with previous studies (Hua et al., 2006; Liu and Croué, 2016). As the Br^- concentration elevated, THM yields increased steadily, reaching 2–4 times at [Br^-]/DOC of 0.4 compared with that at ambient Br^- concentration. For example, increasing the [Br^-]/DOC from ambient level to 0.4, the formation of total THMs from AOM increased from 7.9 to 21.4 μg/mg C, respectively. In the absence of Br^-, only TCM was formed (Appendix A Fig. S1a). Increasing initial Br^- concentration led to less TCM formation, but enhanced the formation of brominated THMs (e.g., TBM). In the presence of Br^-, secondarily formed HOBr can outcompete HOCl to react with DOM due to its higher reaction rate constants compared with that of HOCl with DOM (Criquet et al., 2015). In addition, the larger amount of the weight of bromine atom makes contribution to the higher weight-based concentrations of total DBPs (Hong et al., 2017).

For THM species, TCM was predominant in all samples containing different types of DOM when Br^- concentration was in a low range (Appendix A Fig. S1a). At a [Br^-]/DOC ratio of 0.1 (i.e. [Cl_2]/[Br^-] ≈ 20), the median DCBM and DBCM yields of samples with various DOM were almost equal (AOM: 3.8 vs 4.7 μg/mg C; NOM: 11.1 vs 10.8 μg/mg C; EfOM: 11.1 vs 11.2 μg/mg C), implying that similar THMs precursors exist in different types of DOM and the reactivity of HOBr to form THMs is at least 20 times higher than that of HOCl. When [Br^-]/DOC increased to 0.4, TBM and DBCM were the dominant species in all chlorinated water samples.

Fig. 2a presents the comparison of BSF values for the formed THMs from various types of DOM. BSF values of THM rank as followed: AOM > NOM > EfOM. For example, at ambient Br^- concentration and [Br^-]/DOC ratio of 0.03, the median BSF_{THM} were 0.13 and 0.21 for AOM samples, 0.07 and 0.14 for NOM samples and 0.04 and 0.09 for EfOM samples, respectively. Bromine incorporation into THMs was also enhanced with the elevation of initial Br^- concentration. Increasing the SUVA generally decreased BSF_{THM}. This indicates that bromine preferentially reacts with DOM with low reactivity (e.g., AOM), which can be explained by the difference in the reactivity of chlorine and bromine toward DOM (Liu et al., 2022).

2.1.2. *HAAs*

Similar with trends of THM formation, the highest HAA yields were observed in NOM samples (median: 34.6 μg/mg C at the ambient Br^- level, while those in EfOM and AOM samples were 23.9 and 6.3 μg/mg C, respectively (Fig. 1b). The highest HAA yields were observed in AOM, NOM and EfOM samples with high SUVA and high initial Br^- concentration , indicating that increasing SUVA values tends to enhance the formation of HAAs (Liu and Croué, 2016). Appendix A Table S1 shows that SUVA values of AOM and EfOM samples were much lower than NOM due to their limited amount of humic substances (Westerhoff and Mash, 2002).

Increasing initial Br^- concentration slightly increased the formation of total HAAs. For example, while increasing the

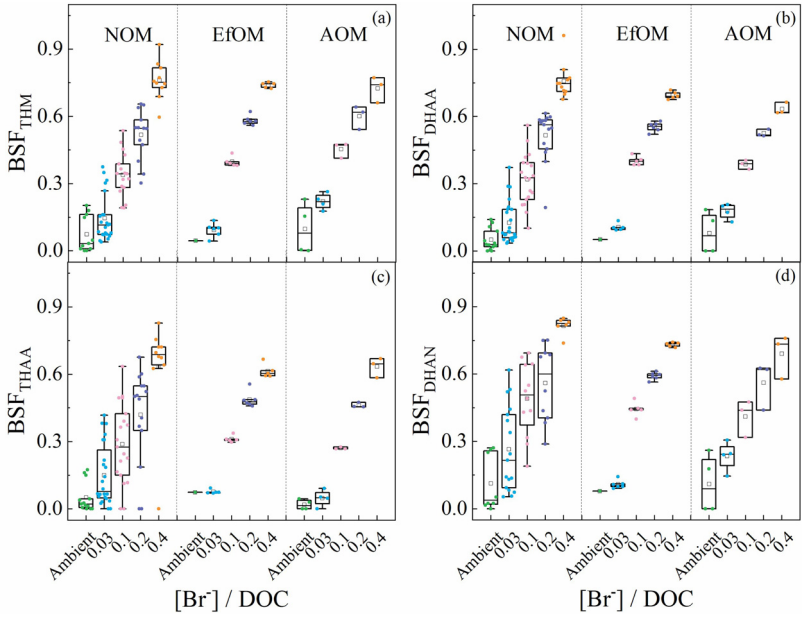

Fig. 2 – Statistical analyses of (a) BSF_{THM}, (b) BSF_{DHAA}, (c) BSF_{THAA} and (d) BSF_{DHAN} of NOM, EfOM and AOM samples under various initial Br^- concentrations based on data collected from literature. Conditions: [HOCl]/DOC = 1.4–3.3 mg Cl_2/ mg C, pH = 7–8, T = 20–25 °C, reaction time = 24 hr.

[Br^-]/DOC from ambient level to 0.4, the total HAA yields increased from 34.6 to 44.8, 23.9 to 49.2 and 6.3 to 7.9 μg/mg C for NOM, EfOM and AOM, respectively. With respect to the speciation of HAAs formed, mono-halogenated acetic acids were minor, although they showed slightly higher formation in EfOM samples (Appendix A Fig. S1b). Di- and tri- halogenated acetic acids were the major species. The latter one showed a higher contribution to the HAA pool (54%–60%, Appendix A Fig. S1c), with stable ratio regardless of initial Br^- concentrations.

BSF values for DHAAs and THAAs increased as initial Br^- concentration increased (Fig. 2b, c). Like BSF_{THM}, BSF_{DHAA} and BSF_{THAA} decreased as SUVA increased, especially when Br^- concentration in a low range. However, when [Br^-]/DOC mass ratio increased to a high range of 0.4 (0.33–0.44), BSF values among different types of DOM presents slight differences (ranging from 0.6 to 0.7), indicating minor effect of DOM types on bromine substitution in the presence of high Br^- concentration.

2.1.3. *HANs*

Different from THMs and HAAs, median levels of HAN yields in AOM and EfOM samples were higher than NOM samples. In the presence of ambient level of Br^- (e.g., [Br^-]/DOC mass ratio = 0–0.01), the highest median value of HAN yields appeared in AOM waters (1.6 μg/mg C). Meanwhile, with low Br^- concentration (e.g., [Br^-]/DOC of 0.03), EfOM samples showed the highest median HAN level (2.7 μg/mg C) among three types of DOM (Fig. 1d). This could be ascribed to higher amounts of N-containing precursors in AOM and EfOM than NOM (Liu et al., 2018;Habip, 2018; Liu et al., 2020). Based on a DBP survey in Europe, the weight ratio of DCAN to TCM was ~10% on a median basis (Krasner et al., 2016), which is consistent with this ratio of NOM from the database regardless of varying Br^- concentrations. However, DCAN/TCM mass ratio witnessed an increasing trend when SUVA decreased, which ranged from 15%–25% and 22%–35% for EfOM and AOM, respectively. This further implies high proportion of N-DBP precursors in EfOM and AOM.

With the increase of initial Br^- concentration, the dominant species of HANs shifted from DCAN to DBAN (Appendix A Fig. S1d). NOM presents the highest HAN yields when initial Br^- concentration was in a high range, which may result from the wide range of SUVA values of NOM samples. Increasing the initial Br^- concentrations also increased the BSF values of DHANs (Fig. 2d). Due to the large amount of NOM samples in the database, BSF_{DHAN} of NOM varied in a wide range. However, it appears that AOM presents higher BSF_{DHAN} especially when Br^- concentration in a relatively low level. For example, BSF_{DHAN} were 0.18 and 0.24 at [Br^-]/DOC mass ratio of 0.03 in NOM and AOM, respectively.

2.1.4. *HALs*

Owing to the insufficient data of HAL formation under various initial Br^- concentrations, only mean HAL yields from different origins of DOM in the presence of ambient Br^- concentration (i.e., [Br^-]/DOC mass ratio of 0–0.01) are shown (Fig. 3a). Mean HAL yields of AOM were comparable with NOM, and both were higher than EfOM samples. This is in line with the finding that HALs are the third most abundant DBPs at DWTPs (Krasner et al., 2006; Lau et al., 2020). Fang et al. (2021) also reported that highly hydrophilic substances considerably served as HAL precursors downstream of the Yangtze River . Our recent study showed a high HAL formation (6.8 μg/mg C) in Suwannee River NOM chlorination experiments (Liu et al., 2022), indicating that humic phenolic moieties could also significantly contribute to the formation of HALs (Chuang et al., 2015).

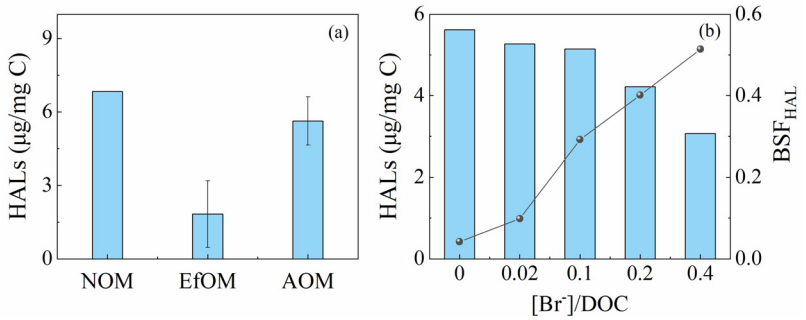

Fig. 3 – (a) Mean HAL yields from different DOM origins during chlorination without additional Br^- in water from literature. (b) Mean HAL yields and BSF_{HAL} of chlorinated AOM waters under various initial Br^- concentrations. Conditions: [HOCl]/DOC = 1.4–3.3 mg Cl_2/ mg C, pH = 7–8, T = 20–25 °C, reaction time = 24 hr.

The formation of HALs and corresponding BSF_{HAL} values during chlorination of AOM in the presence of different initial Br^- concentration are shown in Fig. 3b. In contrast to THMs, as [Br^-]/DOC ratio increased, HAL yields decreased although BSF_{HAL} still increased. It is known that brominated HALs (e.g., tribromo species) are instable and can decompose to the corresponding THMs, resulting in decreased concentration of HALs (Liu et al., 2018). As Appendix A Fig. S2 shows, DCBAL and DBCAL became predominant species when [Br^-]/DOC ratios were ≥0.1.

2.1.5. *HAMs*

Fig. S3 shows the formation of HAMs (mean level) from different types of DOM after chlorination under comparable conditions. As illustrated, different from carbonaceous DBPs (C-DBPs), HAM formation from EfOM samples (mean: 1.3 μg/mg C) ranked the first, followed by NOM and AOM (0.3 and 0.1 μg/mg C, respectively). This may indicate that EfOM which contain high levels of nitrogen-containing moieties may serve as precursors of HAMs (Le Roux et al., 2017; Shao et al., 2020).

2.2. *DBP formation during chloramination and prechlorination-chloramination*

2.2.1. *I-THMs*

Monochloramine can rapidly oxidize iodide to HOI, while it is ineffective in oxidizing HOI to iodate (Bichsel and Von Gunten, 2000). Consequently, higher yields of I-DBPs were observed in chloraminated samples in the presence of I^- compared with chlorinated samples. Fig. 4 shows the formation of I-THMs in NOM and AOM samples during chloramination with various initial I^- concentration. Of note, EfOM data were unavaiable. Significant higher I-THM formation was observed in chloraminated AOM samples in the presence of high level of I^-. For example, the mean I-THM yields of AOM samples reached 77.2 μg/mg C at a [I^-]/DOC ratio of 0.126, while those of NOM samples were 67.3 μg/mg C at a [I^-]/DOC ratio of 0.400. Hydrophilic fractions with low SUVA values may favor the formation of I-DBPs during chloramination (Allard et al., 2015). Our recent study indicated that iodine preferentially reacts with AOM to form TIM (Liu et al., 2022).

For the effect of initial I^- concentration in water, I-THMs apparently increased as [I^-]/DOC ratio increased. Among six

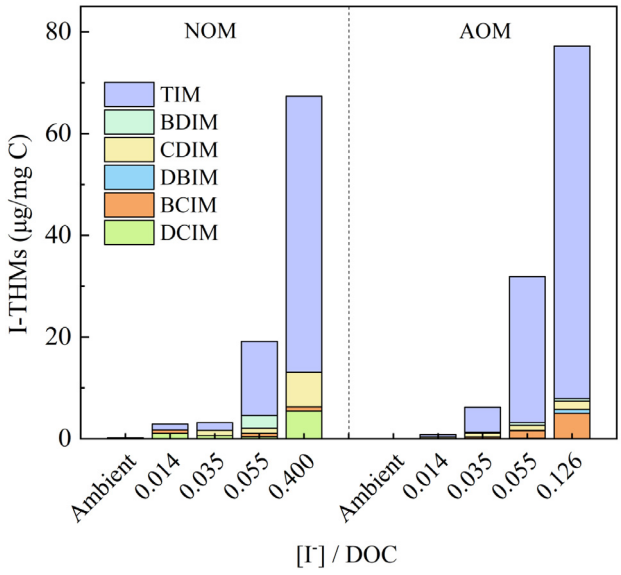

Fig. 4 – Mean I-THM yields in NOM and AOM samples during chloramination under various initial I^- concentrations from literature. Conditions: [NH_2Cl]/DOC = 1.4–3.3 mg Cl_2/ mg C, pH = 7–8, T = 20–25 °C, reaction time = 24 hr .

I-THMs, TIM was the predominant species in all samples because free iodine was the major halogen species (Liu et al., 2019). The percentage of TIM in AOM samples was higher than that in NOM samples. For example, when [I^-]/DOC ratio was 0.03–0.04, the median fraction of TIM over total I-THMs in NOM samples was 42%, while that in AOM samples was 79%. This is probably because iodine preferentially reacts with DOM with low SUVA (Liu et al., 2019).

Apart from preformed monochloramine, NH_2Cl is usually prepared *in situ* at drinking water treatment plants by prechlorination followed by ammonia addition (Deborde and von Gunten, 2008). Fig. 5 shows the I-THM formation with different prechlorination time and various initial I^- concentration. Akin to the I-THM formation in chloramination by preformed chloramine, increasing initial I^- concentration favored the formation of I-THMs and apparently higher I-THM yields appeared in chloraminated AOM samples. Since longer prechlorination

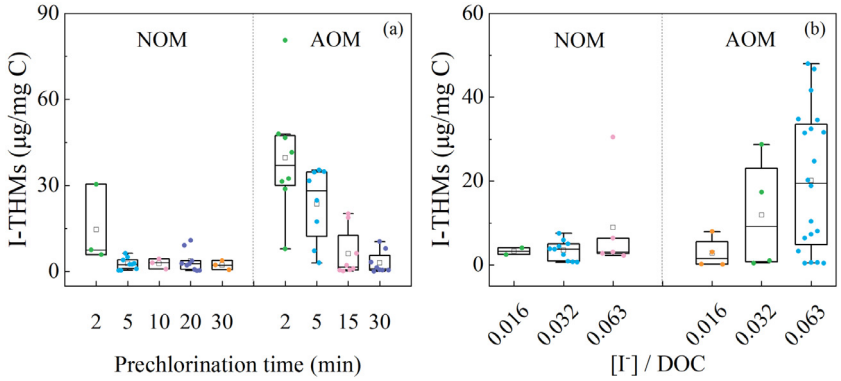

Fig. 5 – Statistical analyses for the yields of I-THMs during prechlorination-chloramination under (a) different prechlorination time and (b) various initial I^- concentrations from literature. Conditions: [NH_2Cl]/DOC = 1.4–3.3 mg Cl_2/ mg C, pH = 7–8, T = 20–25 °C, reaction time = 24 hr.

time can reduce I-DBPs but increase Cl-/Br-DBPs, prechlorination time must be optimized to mitigate the formation of I-DBPs meanwhile control the formation of Cl-/Br-DBPs.

As I^- concentration increased, ISF_{THM} for NOM significantly increased (Appendix A Fig. S4). It almost doubled (0.45 vs. 0.93) when [I^-]/DOC increased from 0.035 to 0.055. In contrast to NOM, ISF_{THM} for AOM reached 0.87 when [I^-]/DOC mass ratio was 0.010. Afterwards, it slightly increased, ranging from 0.91 to 0.98, as I^- concentration increased. Increasing the SUVA values generally decreased ISF_{THM} due to iodine being more prone to react with DOM with low reactivities.

2.2.2. *THMs*

Formation of THMs from NOM, EfOM and AOM samples during chloramination in the presence of Br^- was shown in Appendix A Figs. S5 and S6. Concentrations of THMs in chloraminated AOM samples were below detection limits. Under similar conditions, concentrations of THMs in chloraminated samples were substantially lower than those in chlorinated samples. For example, THM yields of chlorinated NOM samples with ambient Br^- level varied from 4.5 to 17.0 μg/mg C, while that of chloraminated NOM samples was <1.0 μg/mg C. Although only limited EfOM data were available, slightly higher THM yields were observed in chloraminated EfOM waters compared to NOM waters at a [Br^-/DOC] of 0.03. Other than chlorination, increasing initial Br^- concentration only slightly increased THM formation during chloramination probably due to the limited concentration of free bromine (Liu et al., 2019).

2.2.3. *I-HAAs*

During chloramination, I-THMs can be formed in high concentrations in the presence of I^-, but this was not the case for I-HAAs. As shown in Appendix A Fig. S7a, I-HAA yields were both <0.3 μg/mg C in NOM and AOM during chloramination at 1 μmol/L of I^-. Based on the I-DBP occurrence study conducted by Richardson et al. (2008), there was a fair level of association between I-THMs vs I-HAAs (Appendix A Fig. S7b). According to the slope (i.e., 20.82), the formation of I-THMs was c.a. 20 times higher than I-HAAs. This was in agreement with our findings obtained from NOM and AOM (Liu et al., 2022). In addition, I-HAA concentrations from NOM and AOM were comparable, which indicated that AOM served as important I-THM precursors but not I-HAA precursors. This implied the different formation pathways of I-THMs and I-HAAs. HAA formation requires oxidizable functional groups, whereas THMs can be formed via hydrolysis pathways. Since iodine is a weak oxidant, other than I-HAAs, I-THMs were preferentially produced by HOI during chloramination process.

2.2.4. *HAAs*

Similar to THMs, significantly lower concentrations of HAAs were observed in chloraminated NOM samples compared with chlorinated NOM waters (Appendix A Figs. S5 and S6). When concentrations of Br^- was in a low range ([Br^-/DOC] = 0–0.3), HAA yields in NOM samples varied from 0.8 to 7.7 μg/mg C. Significantly lower HAA yields were observed in AOM samples during chloramination compared to chlorination as well (Appendix A Fig. S6). In addition, increasing initial Br^- concentration slightly increased HAA formation for NOM.

2.2.5. *HANs*

The median value of HAN yields was 0.1 μg/mg C in chloraminated NOM waters at [Br^-]/DOC mass ratios of 0–0.01, which was more than 10 times lower than that in chlorination (Appendix A Fig. S5). HAN concentrations were below detection limits in reported chloraminated AOM samples, whereas HAN data from EfOM were insufficient. Compared with THMs and HAAs, increasing Br^- visibly enhanced HAN formation in chloraminated NOM waters. Increasing initial Br^- concentration from ambient level to [Br^-]/DOC of 0.2 gives an increase in median HAN yields from 0.1 to 0.4 μg/mg C.

2.2.6. *HALs*

HAL formation in chloramination is minor, ranging from 0–0.5 μg/mg C for AOM and NOM because of limited chlorine exposure. While prechlorination was placed prior to chloramination process, increasing prechlorination time increased HAL concentrations. During prechlorination, AOM favored HAL formation when compared to NOM. For example, 3.0 μg/mg C of total HALs were formed in AOM samples at a prechlorination time of 30 min, while those in NOM samples were about

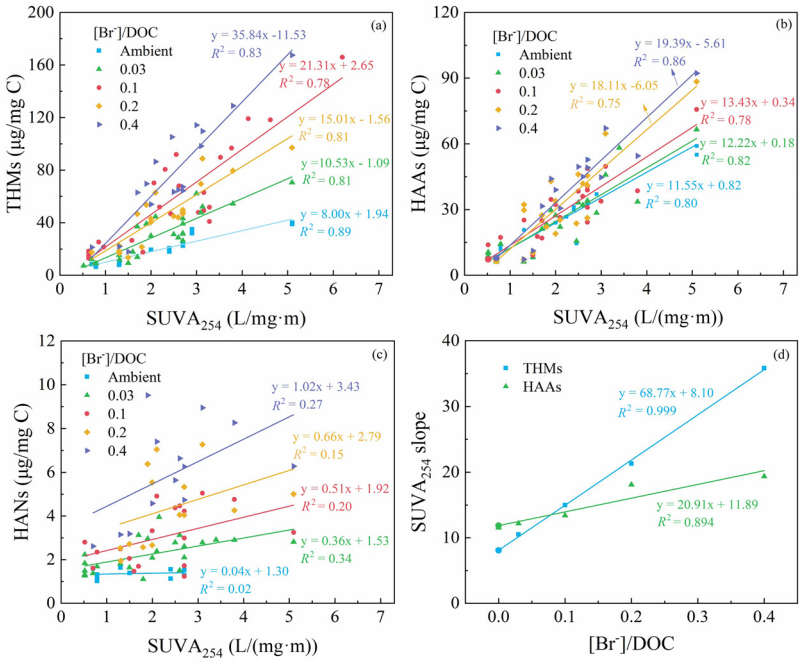

Fig. 6 – Linear regressions between (a) THMs and $SUVA_{254}$, (b) HAAs and $SUVA_{254}$, (c) HANs and $SUVA_{254}$, (d) slopes of DBPs vs. $SUVA_{254}$ and initial Br^- concentrations in chlorination conditions based on data collected from literature. Conditions: [HOCl]/DOC = 1.4–3.3 mg Cl_2/ mg C, pH = 7–8, T = 20–25 °C, reaction time = 24 hr.

0.9 μg/mg C. This agrees with the observation during chlorination. In addition, low SUVA preferentially formed Br-HALs during chloramination in the presence of Br^- (Liu et al., 2022).

2.2.7. *HAMs*

Most of the studies for chloramination were performed in formation potential (FP) conditions (high dose of chloramine or long reaction time) (Huang et al., 2017; Zhang et al., 2017). Nevertheless, it was unpractical for realistic conditions. Based on the formation pathways of HAMs, it can be expected that concentrations of HAMs were comparable with HANs. Both were lower in chloramination than those in chlorination conditions.

2.3. *Regression analysis*

Based on the data collected, the formation of THMs, HAAs, HANs, HALs, and HAMs was plotted as a function of $SUVA_{254}$ (Figs. 6 and Appendix A Fig. S8). THM formation and $SUVA_{254}$ showed strong associations (i.e., $R^2 = 0.78–0.89$) for all Br^- concentrations (Fig. 6a). The slope of the linear regression steadily increased with an increase in initial Br^- concentrations, indicating the higher reactivity of HOBr than HOCl to react with DOM. Similar trends were observed for HAAs as well, however, its slope only slightly increased with the increase of Br^- concentration (Fig. 6b). High association between HAL formation and $SUVA_{254}$ ($R^2 = 0.86$) were also observed at $[Br^-]$/DOC mass ratio of 0.2 (Appendix A Fig. S8), showing the contribution of phenolic substances to HAL formation. In contrast to C-DBPs, a weak relationship was observed for N-DBP (HAN and HAM) formation with $SUVA_{254}$ (Figs. 6c and Appendix A Fig. S8).

The relationship of Br^- concentration with the $SUVA_{254}$ slope (Fig. 6a–c) was further analyzed to examine the effect of Br^- concentration on DBP formation (Fig. 6d). Regressions between Br^- concentration and slopes of THMs and HAAs (i.e., $R^2 = 0.999$ and 0.894, respectively) indicated that Br^- concentration played an important role on DBP formation. The rank order of the regression slope (i.e., THMs > HAAs) was consistent with the formed DBP concentration during chlorination. The relationships between DON and the formation of HAN and HAM during chlorination and chloramination were weak (Appendix A Fig. S9), indicating that the precursors of N-DBPs were complex and diverse. Therefore, correlation analyses between DOM characteristics and N-DBP formation warrant further investigation.

3. Conclusion

The impact of Br^- and I^- on the formation of THMs, HAAs, HANs, HALs and HAMs during chlorination and chloramination under comparable conditions were analyzed from various origins of DOM. Due to high fractions of phenolic compounds, NOM presents the highest reactivity with both chlorine and monochloramine, thereby forming the highest levels of THMs and HAAs. When the initial Br^- concentration was in a low range (i.e. $[Br^-]$/DOC = 0.0–0.04), BSF values decreased as SUVA increased. However, the effect of DOM types on BSF values was minor in the presence of high Br^- concentration. Increasing the initial Br^- concentration, THM, HAA, HAN and HAM formation increased, whereas HAL concentrations decreased. Chloramination significantly mitigate the formation of Cl-/Br-DBPs. However, I-THM formation was observed in chlorami-

nated samples in the presence of I^-. The formation of I-THMs in the presence of AOM was higher than that of NOM, probably because iodine preferentially reacts with DOM with low SUVA. As DBPs are considered as important drivers for the toxicity of disinfected waters, further investigation of toxicity of disinfected water containing various types of DOM is required.

Acknowledgments

This study was partially supported by the Key Laboratory of Drinking Water Science and Technology of Chinese Academy of Sciences (No. 20Z01KLDWST).

Appendix A Supplementary data

Supplementary material associated with this article can be found, in the online version, at doi:10.1016/j.jes.2022.04.014.

REFERENCES

Allard, S., Tan, J., Joll, C.A., von Gunten, U., 2015. Mechanistic study on the formation of Cl-/Br-/I-trihalomethanes during chlorination/chloramination combined with a theoretical cytotoxicity evaluation. Environ. Sci. Technol. 49, 11105–11114.

Aziz, M.T., Granger, C.O., Westerman, D.C., Putnam, S.P., Ferry, J.L., Richardson, S.D., 2022. Microseira wollei and phormidium algae more than doubles DBP concentrations and calculated toxicity in drinking water. Water Res., 118316.

Bellar, T.A., Lichtenberg, J.J., Kroner, R.C., 1974. The occurrence of organohalides in chlorinated drinking waters. J. Am. Water Works Assoc. 66, 703–706.

Bichsel, Y., Von Gunten, U., 2000. Formation of iodo-trihalomethanes during disinfection and oxidation of iodide-containing waters. Environ. Sci. Technol. 34, 2784–2791.

Chapra, S.C., Boehlert, B., Fant, C., Bierman, V.J., Henderson, J., Mills, D., et al., 2017. Climate change impacts on harmful algal blooms in U.S. freshwaters: a screening-level assessment. Environ. Sci. Technol. 51, 8933–8943.

Chuang, Y.H., McCurry, D.L., Tung, H-h, Mitch, W.A., 2015. Formation pathways and trade-offs between haloacetamides and haloacetaldehydes during combined chlorination and chloramination of lignin phenols and natural waters. Environ. Sci. Technol. 49, 14432–14440.

Chuang, Y.H., Mitch, W.A., 2017. Effect of ozonation and biological activated carbon treatment of wastewater effluents on formation of *N* -nitrosamines and halogenated disinfection byproducts. Environ. Sci. Technol. 51, 2329–2338.

Cowman, G.A., Singer, P.C., 1996. Effect of bromide ion on haloacetic acid speciation resulting from chlorination and chloramination of aquatic humic substances. Environ. Sci. Technol. 30, 16–24.

Criquet, J., Rodriguez, E.M., Allard, S., Wellauer, S., Salhi, E., Joll, C.A., et al., 2015. Reaction of bromine and chlorine with phenolic compounds and natural organic matter extracts – electrophilic aromatic substitution and oxidation. Water Res. 85, 476–486.

Deborde, M., von Gunten, U., 2008. Reactions of chlorine with inorganic and organic compounds during water treatment—kinetics and mechanisms: a critical review. Water Res. 42, 13–51.

Elimelech, M., Phillip, W.A., 2011. The future of seawater desalination: energy, technology, and the environment. Science 333, 712–717.

Eom, H., Borgatti, D., Paerl, H.W., Park, C., 2017. Formation of low-molecular-weight dissolved organic nitrogen in predenitrification biological nutrient removal systems and its impact on eutrophication in coastal waters. Environ. Sci. Technol. 51, 3776–3783.

Ersan, M.S., Liu, C., Amy, G., Karanfil, T., 2019a. The interplay between natural organic matter and bromide on bromine substitution. Sci. Total Environ. 646, 1172–1181.

Ersan, M.S., Liu, C., Amy, G., Plewa, M.J., Wagner, E.D., Karanfil, T., 2019b. Chloramination of iodide-containing waters: formation of iodinated disinfection byproducts and toxicity correlation with total organic halides of treated waters. Sci. Total Environ. 697, 134142.

Fang, C., Yang, X., Ding, S., Luan, X., Xiao, R., Du, Z., et al., 2021. Characterization of dissolved organic matter and its derived disinfection byproduct formation along the Yangtze river. Environ. Sci. Technol. 55, 12326–12336.

Good, K.D., VanBriesen, J.M., 2016. Current and potential future bromide loads from coal-fired power plants in the allegheny river basin and their effects on downstream concentrations. Environ. Sci. Technol. 50, 9078–9088.

Habip, N, 2018. Formation and speciation of disinfection by-products in treated wastewater effluent during chlorination. MS Thesis Clemson University, USA. https://tigerprints.clemson.edu/all_theses/2986.

Henderson, R.K., Baker, A., Parsons, S.A., Jefferson, B., 2008. Characterisation of algogenic organic matter extracted from cyanobacteria, green algae and diatoms. Water Res. 42, 3435–3445.

Her, N., Amy, G., Park, H.R., Song, M., 2004. Characterizing algogenic organic matter (AOM) and evaluating associated NF membrane fouling. Water Res. 38, 1427–1438.

Hong, H., Yan, X., Song, X., Qin, Y., Sun, H., Lin, H., et al., 2017. Bromine incorporation into five DBP classes upon chlorination of water with extremely low SUVA values. Sci. Total Environ. 590-591, 720–728.

Hua, G., Reckhow, D.A., Kim, J., 2006. Effect of bromide and iodide ions on the formation and speciation of disinfection byproducts during chlorination. Environ. Sci. Technol. 40, 3050–3056.

Huang, H., Chen, B.Y., Zhu, Z.R., 2017. Formation and speciation of haloacetamides and haloacetonitriles for chlorination, chloramination, and chlorination followed by chloramination. Chemosphere 166, 126–134.

Jeong, C.H., Postigo, C., Richardson, S.D., Simmons, J.E., Kimura, S.Y., Mariñas, B.J., et al., 2015. Occurrence and comparative toxicity of haloacetaldehyde disinfection byproducts in drinking water. Environ. Sci. Technol. 49, 13749–13759.

Jones, D.B., Saglam, A., Song, H., Karanfil, T., 2012. The impact of bromide/iodide concentration and ratio on iodinated trihalomethane formation and speciation. Water Res. 46, 11–20.

Kanan, A., Karanfil, T., 2020. Estimation of haloacetonitriles formation in water: uniform formation conditions versus formation potential tests. Sci. Total Environ. 744, 140987.

Krasner, S.W., Kostopoulou, M., Toledano, M.B., Wright, J., Patelarou, E., Kogevinas, M., et al., 2016. Occurrence of DBPs in drinking water of european regions for epidemiology studies. J. Am. Water Works Assoc. 108, E501–E512.

Krasner, S.W., Weinberg, H.S., Richardson, S.D., Pastor, S.J., Chinn, R., Sclimenti, M.J., et al., 2006. Occurrence of a new generation of disinfection byproducts. Environ. Sci. Technol. 40, 7175–7185.

Kumar, K., Margerum, D.W., 1987. Kinetics and mechanism of general-acid-assisted oxidation of bromide by hypochlorite and hypochlorous acid. Inorg. Chem. 26, 2706–2711.
Lau, S.S., Wei, X., Bokenkamp, K., Wagner, E.D., Plewa, M.J., Mitch, W.A., 2020. Assessing additivity of cytotoxicity associated with disinfection byproducts in potable reuse and conventional drinking waters. Environ. Sci. Technol. 54, 5729–5736.
Le Roux, J., Plewa, M.J., Wagner, E.D., Nihemaiti, M., Dad, A., Croué, J.P., 2017. Chloramination of wastewater effluent: toxicity and formation of disinfection byproducts. J. Environ. Sci. 58, 135–145.
Lee, W., Westerhoff, P., 2006. Dissolved organic nitrogen removal during water treatment by aluminum sulfate and cationic polymer coagulation. Water Res. 40, 3767–3774.
Leenheer, J.A., Croué, J.P., 2003. Peer reviewed: characterizing aquatic dissolved organic matter. Environ. Sci. Technol. 37, 18A–26A.
Liu, C., 2021. The role of metal oxides on oxidant decay and disinfection byproduct formation in drinking waters: relevance to distribution systems. J. Environ. Sci. 110, 140–149.
Liu, C., Croué, J.P., 2016. Formation of bromate and halogenated disinfection byproducts during chlorination of bromide-containing waters in the presence of dissolved organic matter and CuO. Environ. Sci. Technol. 50, 135–144.
Liu, C., Ersan, M.S., Plewa, M.J., Amy, G., Karanfil, T., 2018. Formation of regulated and unregulated disinfection byproducts during chlorination of algal organic matter extracted from freshwater and marine algae. Water Res. 142, 313–324.
Liu, C., Ersan, M.S., Plewa, M.J., Amy, G., Karanfil, T., 2019. Formation of iodinated trihalomethanes and noniodinated disinfection byproducts during chloramination of algal organic matter extracted from microcystis aeruginosa. Water Res. 162, 115–126.
Liu, C., Ersan, M.S., Wagner, E., Plewa, M.J., Amy, G., Karanfil, T., 2020. Toxicity of chlorinated algal-impacted waters: formation of disinfection byproducts vs. reduction of cyanotoxins. Water Res. 184, 116145.
Liu, C., Salhi, E., Croué, J.P., von Gunten, U., 2014. Chlorination of iodide-containing waters in the presence of CuO: formation of periodate. Environ. Sci. Technol. 48, 13173–13180.
Liu, C., Shin, Y.H., Wei, X., Ersan, M.S., Wagner, E., Plewa, M.J., et al., 2022. Preferential halogenation of algal organic matter by iodine over chlorine and bromine: formation of disinfection byproducts and correlation with toxicity of disinfected waters. Environ. Sci. Technol. 56, 1244–1256.
Ministry of Environment of Korea, 2020. Drinking Water Management Act. Ministry of Environment of Korea.
Ministry of Health of Japan, 2015. Drinking Water Quality Standards in Japan. Ministry of Health of Japan.
Ministry of Health of the PR China, 2022. Standards for Drinking Water Quality (GB 5749–2022). China Standard Press Beijing.
Mitch, W.A., Krasner, S.W., Westerhoff, P.A.D., 2009. Occurrence and Formation of Nitrogenous Disinfection By-Products. AWWA Research Foundation, Denver, CO Products.
Muellner, M.G., Wagner, E.D., McCalla, K., Richardson, S.D., Woo, Y.T., Plewa, M.J., 2007. Haloacetonitriles vs. regulated haloacetic acids: are nitrogen-containing DBPs more toxic? Environ. Sci. Technol. 41, 645–651.
Plewa, M.J., Simmons, J.E., Richardson, S.D., Wagner, E.D., 2010. Mammalian cell cytotoxicity and genotoxicity of the haloacetic acids, a major class of drinking water disinfection by-products. Environ. Mol. Mutagen. 51, 871–878.
Richardson, S.D., Fasano, F., Ellington, J.J., Crumley, F.G., Buettner, K.M., Evans, J.J., et al., 2008. Occurrence and mammalian cell toxicity of iodinated disinfection byproducts in drinking water. Environ. Sci. Technol. 42, 8330–8338.
Richardson, S.D., Plewa, M.J., 2020. To regulate or not to regulate? What to do with more toxic disinfection by-products? J. Environ. Chem. Eng. 8, 103939.
Richardson, S.D., Plewa, M.J., Wagner, E.D., Schoeny, R., DeMarini, D.M., 2007. Occurrence, genotoxicity, and carcinogenicity of regulated and emerging disinfection by-products in drinking water: a review and roadmap for research. Mutat. Res. Rev. Mutat. Res. 636, 178–242.
Rook, J.J., 1974. Formation of haloforms during chlorination of natural water. Water Treat. Exam. 23, 234–243.
Shao, K.L., Ye, Z.X., Huang, H., Yang, X., 2020. ClO_2 pre-oxidation impacts the formation and nitrogen origins of dichloroacetonitrile and dichloroacetamide during subsequent chloramination. Water Res. 186, 116313.
Shon, H.K., Vigneswaran, S., Snyder, S.A., 2006. Effluent organic matter (EfOM) in wastewater: constituents, effects, and treatment. Crit. Rev. Environ. Sci. Technol. 36, 327–374.
Sirivedhin, T., Gray, K.A., 2005. 2. Comparison of the disinfection by-product formation potentials between a wastewater effluent and surface waters. Water Res. 39, 1025–1036.
USEPA, 2006. Stage 2 disinfectants and disinfection byproducts rule: national primary and secondary drinking water regulations: final rule.
Watson, K., Farré, M.J., Knight, N., 2012. Strategies for the removal of halides from drinking water sources, and their applicability in disinfection by-product minimisation: a critical review. J. Environ. Manag. 110, 276–298.
Wei, X., Yang, M., Zhu, Q., Wagner, E.D., Plewa, M.J., 2020. Comparative quantitative toxicology and QSAR modeling of the haloacetonitriles: forcing agents of water disinfection byproduct toxicity. Environ. Sci. Technol. 54, 8909–8918.
Westerhoff, P., Mash, H., 2002. Dissolved organic nitrogen in drinking water supplies: a review. J. Water Supply Res. Technol. Aqua 51, 415–448.
WHO, 2006. Guidelines for Drinking Water. WHO.
Widrig, D.L., Gray, K.A., McAuliffe, K.S., 1996. Removal of algal-derived organic material by preozonation and coagulation: monitoring changes in organic quality by pyrolysis-GC-MS. Water Res. 30, 2621–2632.
Zhang, N., Liu, C., Qi, F., Xu, B., 2017. The formation of haloacetamides, as an emerging class of N-DBPs, from chlor(am)ination of algal organic matter extracted from *Microcystis aeruginosa*, *Scenedesmus quadricauda* and *Nitzschia palea*. RSC Adv. 7, 7679–7687.